Supplemental Table 1. List of antibodies used in this study.

Antibody	Type	Source	Catalog	RRID	WB dilution	IF dilution
AKT	Mouse monoclonal	Cell Signaling	2920	AB_1147620	1:2000	
AMPK	Rabbit polyclonal	Cell Signaling	2532	AB_330331	1:1000	
β-actin	Mouse monoclonal	Sigma	A5441	AB_476744	1:10000	
BRN3	Goat polyclonal	Santa Cruz	SC-6026	AB_673441		1:200
CHX10	Goat polyclonal	Santa Cruz	SC-21690	AB_2216006		1:200
CTIP2	Rat monoclonal	Abcam	Ab18465	AB_2064130		1:500
LAMP1	Rabbit monoclonal	Cell Signaling	9091	AB_2687579	1:1000	
LAMP1	Rat monoclonal	DSHB	1D4B	AB_2134500	1:200	1:20
LC3 A/B	Rabbit monoclonal	Cell Signaling	12741	AB_2617131	1:1000	
MAP1LC3A	Rabbit monoclonal	Abcam	ab185036	AB_881226		1:200
MAP2	Mouse monoclonal	Synaptic Systems	188011	AB_11042001		1:200
OPTN	Rabbit polyclonal	Novus	NBP1-84682	AB_11032496	1:1000	1:200
OTX2	Goat polyclonal	R&D Systems	AF1979	AB_2157172		1:2000
p62	Mouse monoclonal	Abcam	ab56416	AB_945626	1:2000	1:50
pAKT	Rabbit monoclonal	Cell Signaling	4060	AB_2315049	1:2000	
pAMPK	Rabbit monoclonal	Cell Signaling	2535	AB_331250	1:1000	
pS6	Rabbit polyclonal	Cell Signaling	2215	AB_331682	1:1000	1:200
RBPMS	Guinea pig polyclonal	PhosphoSolutions	1832-RBPMS	AB_2492226		1:500
RFP	Rabbit polyclonal	Rockland	600-401-379	AB_2209751		1:200
RFP	Goat polyclonal	Origene	AB1140-100	AB_2877097		1:200
RFP	Mouse monoclonal	Rockland	200-301-379	AB_2611063		1:200
S6	Rabbit monoclonal	Cell Signaling	2217	AB_331355	1:1000	
Tubulin,β-III	Rabbit polyclonal	Biolegend	802001	AB_2564645		1:500

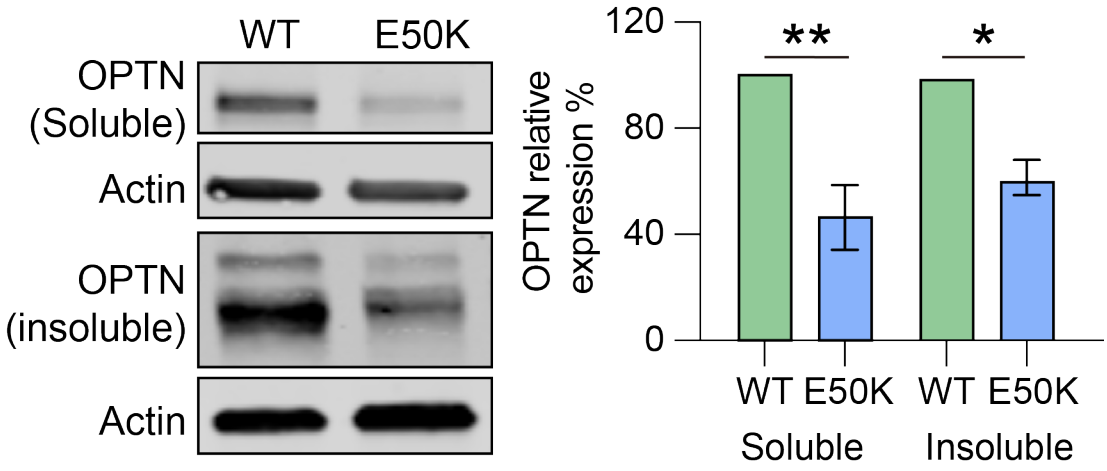

Figure S1. Reduction of OPTN protein was observed in both soluble and insoluble protein fractions. Western blot of OPTN relative to β-actin in isogenic wild type control (WT) and OPTN(E50K) demonstrated a significant reduction in both soluble and insoluble fractions.

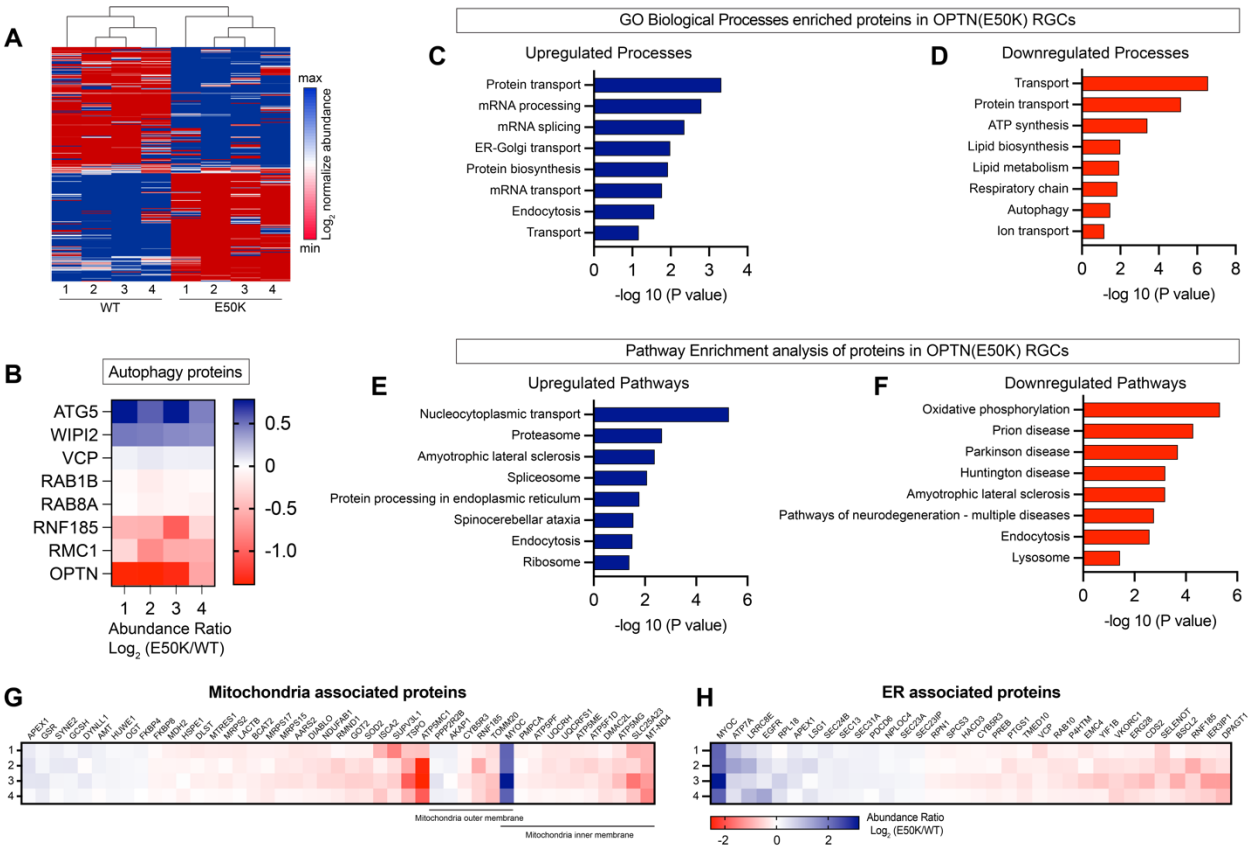

Figure S2. Proteomics analysis of OPTN(E50K) RGCs compared to isogenic control RGCs. (A) Overall heatmap representation of protein expression in isogenic control (WT) and OPTN(E50K) RGCs. (B) Heatmap of differentially expressed autophagy-related genes between isogenic control and OPTN(E50K) RGCs. (C-D) Differentially expressed GO Biological Processes based upon proteomics analysis. (E-F) Differentially expressed pathways by Pathway Enrichment analysis between isogenic control and OPTN(E50K) RGCs. (G-H) Heatmaps detailing the differential expression of genes associated with mitochondrial (G) and endoplasmic reticulum (H) function.

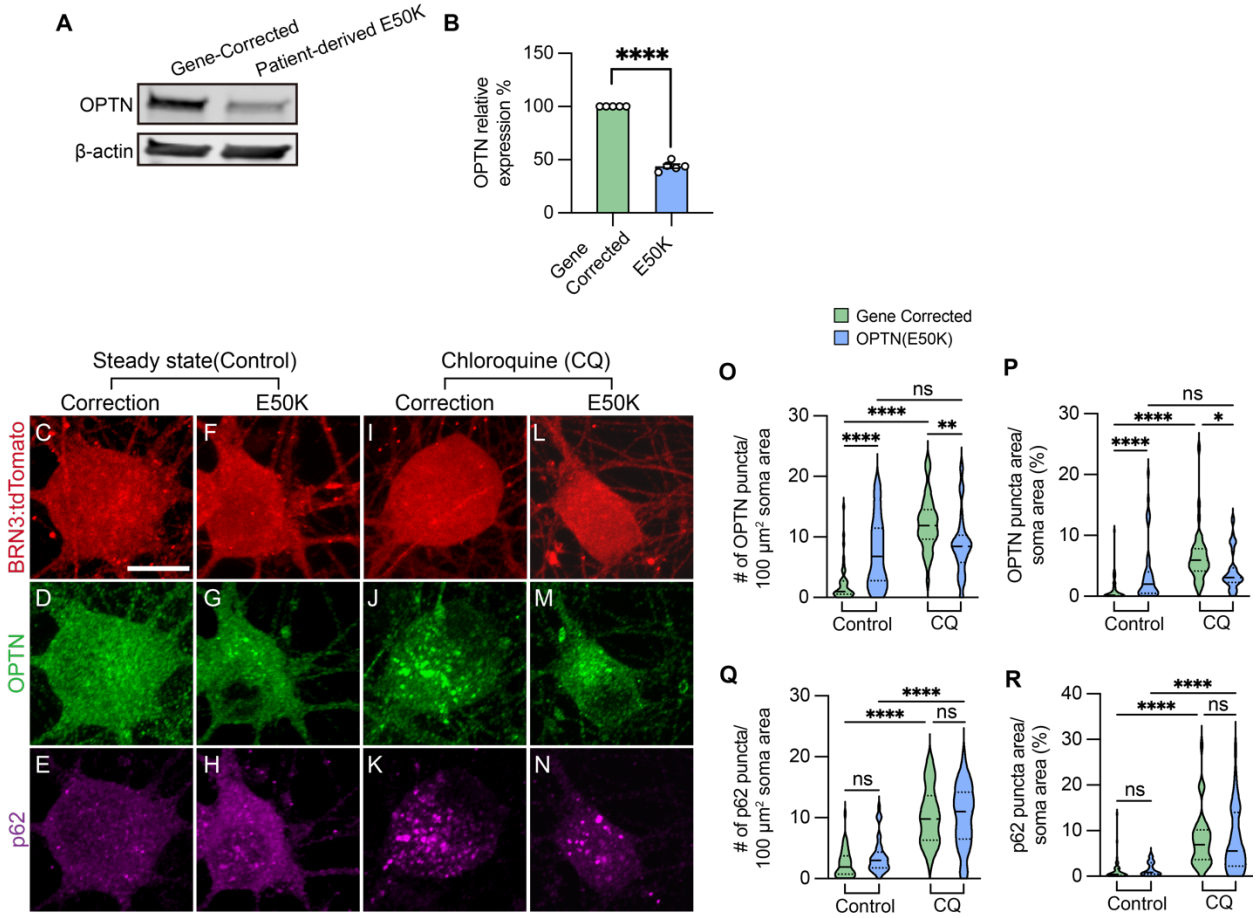

Figure S3. Confirmation of changes in OPTN levels in RGCs derived from patient-specific iPSCs with OPTN(E50K) mutation compared to corresponding isogenic control line. (**A-B**) Western blot of OPTN relative to β-actin in patient-derived OPTN(E50K) and gene-corrected isogenic control iPSC-RGCs (n=5 for each WT and E50K; t-test, ****p<0.0001). (**C-N**) Immunostaining revealed the aggregation of OPTN and p62 puncta in BRN3:tdTomato iPSC-RGCs in patient-derived OPTN(E50K) mutant and gene-corrected isogenic control lines after steady state (control) (C-H) and chloroquine (CQ) treatment (I-N). Scale bar: 10 µm. (**O-R**) Quantification of OPTN puncta (O and P) or p62 puncta (Q and R) in iPSC-RGC (n=3 biological replicates using Ctrl-WT n=42, Ctrl-E50K n=39, CQ-WT n=38 and CQ-E50K n=40 technical replicates; One-way ANOVA, Tukey post hoc test. ****p<0.0001, **p<0.01, *p<0.05, ns= not significant). Data are all represented as mean values ± SEM.

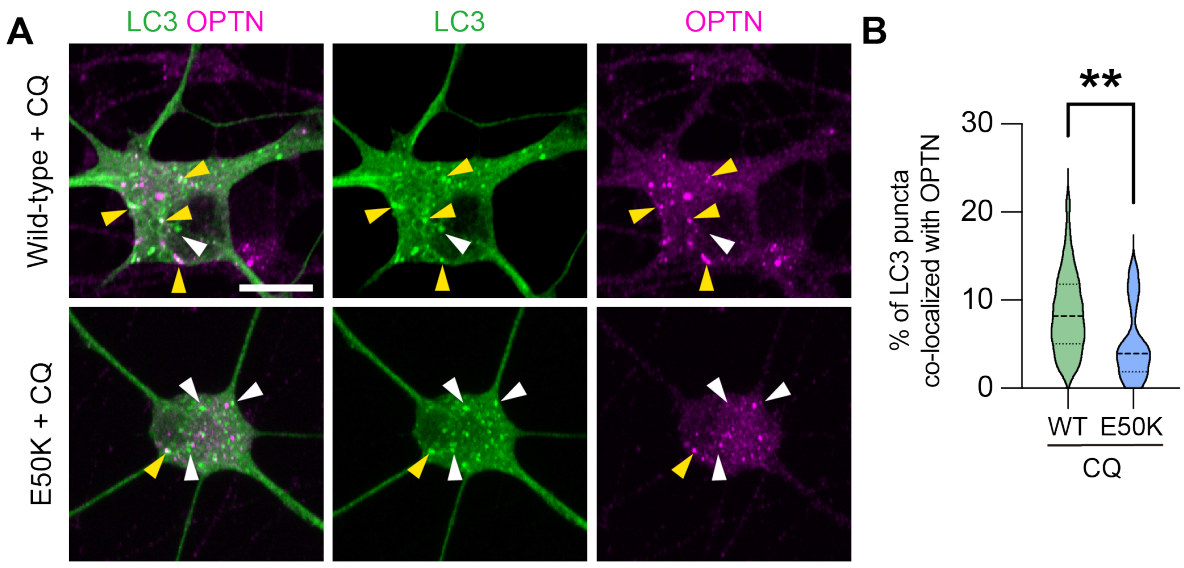

Figure S4. Confirmation of reduced recruitment of LC3 by OPTN in OPTN(E50K) hPSC-RGCs.

(**A**) Representative images of OPTN and LC3 localization in hPSC-RGCs from wild-type and OPTN(E50K) cell lines after chloroquine treatment, in reference to data presented in Figure 2. Yellow arrows label the colocalization between OPTN and LC3 puncta, and white arrows represented that the LC3 puncta did not colocalize with OPTN. Quantification of colocalization between OPTN and LC3 in hPSC-RGCs (n=3 biological replicates using WT n=37 and E50K n=28 technical replicates; t-test, **p>0.005). Scale bar: 10 μm. (**B**) Quantification the number of LC3 puncta per cell body in hPSC-RGCs following chloroquine treatment. Data are represented as mean values ± SEM.

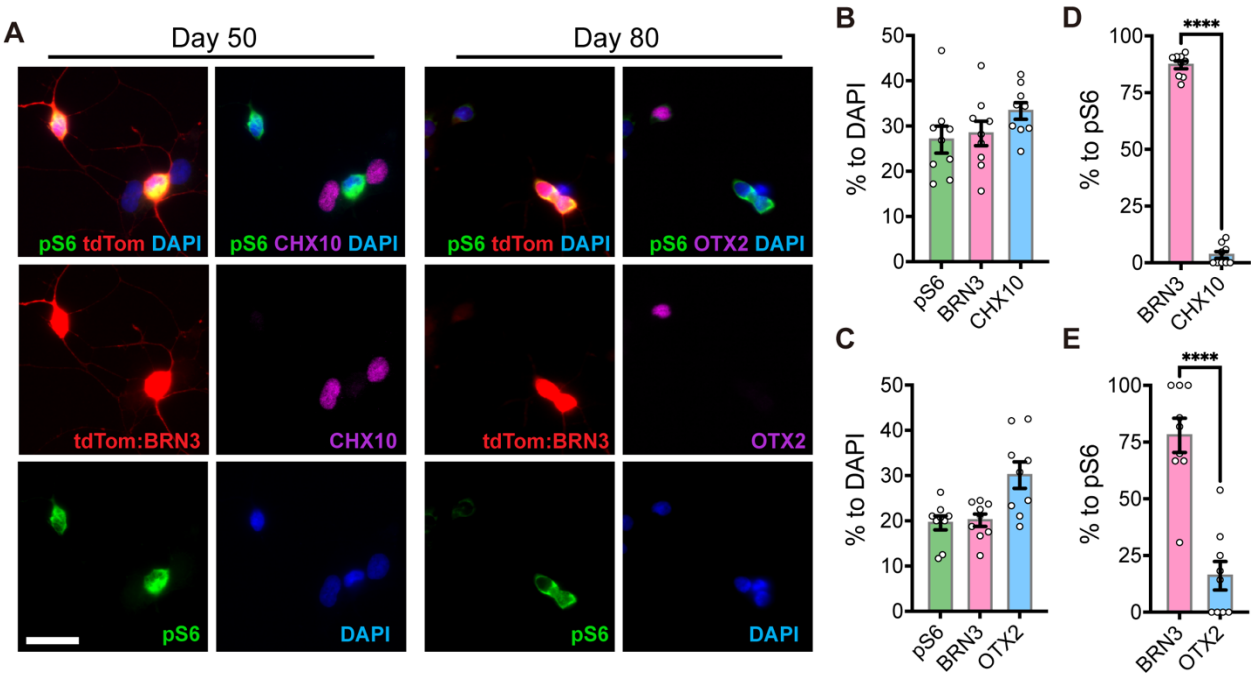

Figure S5. mTORC1 activity is preferentially observed within RGCs among hPSC-derived retinal cells.

(**A**) Retinal organoids were dissociated and plated onto laminin-coated coverslips at either day 50 or day 80 of differentiation to acquire the majority of major retinal cell types, including RGCs (BRN3:tdTomato), retinal progenitor cells (CHX10), and photoreceptors (OTX2), following by analysis of mTORC1 activity based upon co-staining with pS6Ser240/244. Scale bar: 25 μm. (**B-C**) Quantification of results showing the percentage of retinal cell types observed at day 50 or day 80 (n=9 images from three technical replicates). (**D-E**) Quantification of pS6Ser240/244 expression colocalized with either BRN3B:tdTomato, CHX10 or OTX2, suggesting that mTORC1 signaling is highly expressed in RGCs, with little expression in retinal progenitor cells or photoreceptors (n=9 images from three technical replicates; t-test, BRN3 vs CHX10: $p<0.0001$, BRN3 vs OTX2: $p<0.0001$). Data are all represented as mean values ± SEM.

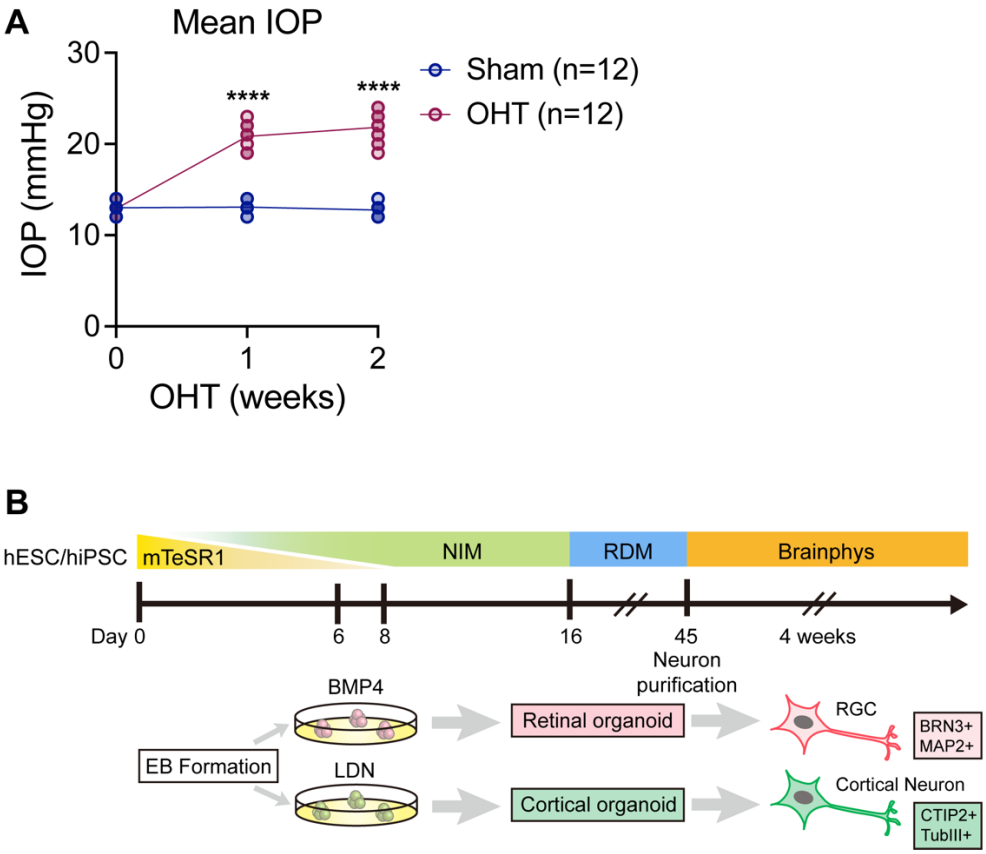

Figure S6. The ocular hypertension mouse and hPSC-RGC OPTN(E50K) models associated with glaucoma.
(**A**) Maintained elevation of intraocular pressure in mouse eyes following the injection of magnetic microbeads into the mouse anterior chamber, compared to sham-injected controls. Two-way ANOVA with Tukey's multiple comparison pos hoc test, ****$p < 0.0001$, $n = 12$ mice/group (**B**) Schematic diagram outlining the differentiation of RGCs and cortical neurons from hPSCs.

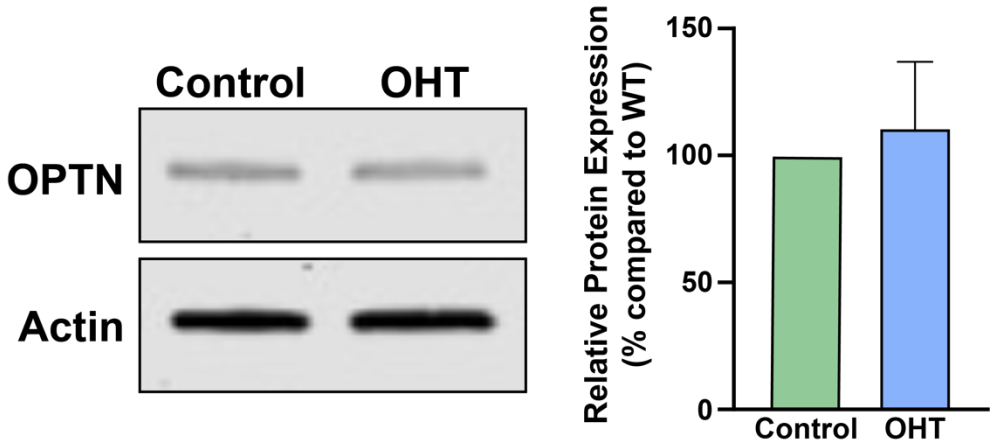

Figure S7. Analysis of OPTN protein expression levels in OHT mouse retina.
Western blot analysis of OPTN protein in OHT mouse retina compared to control demonstrated no significant difference in expression of OPTN due to the ocular hypertensive condition.

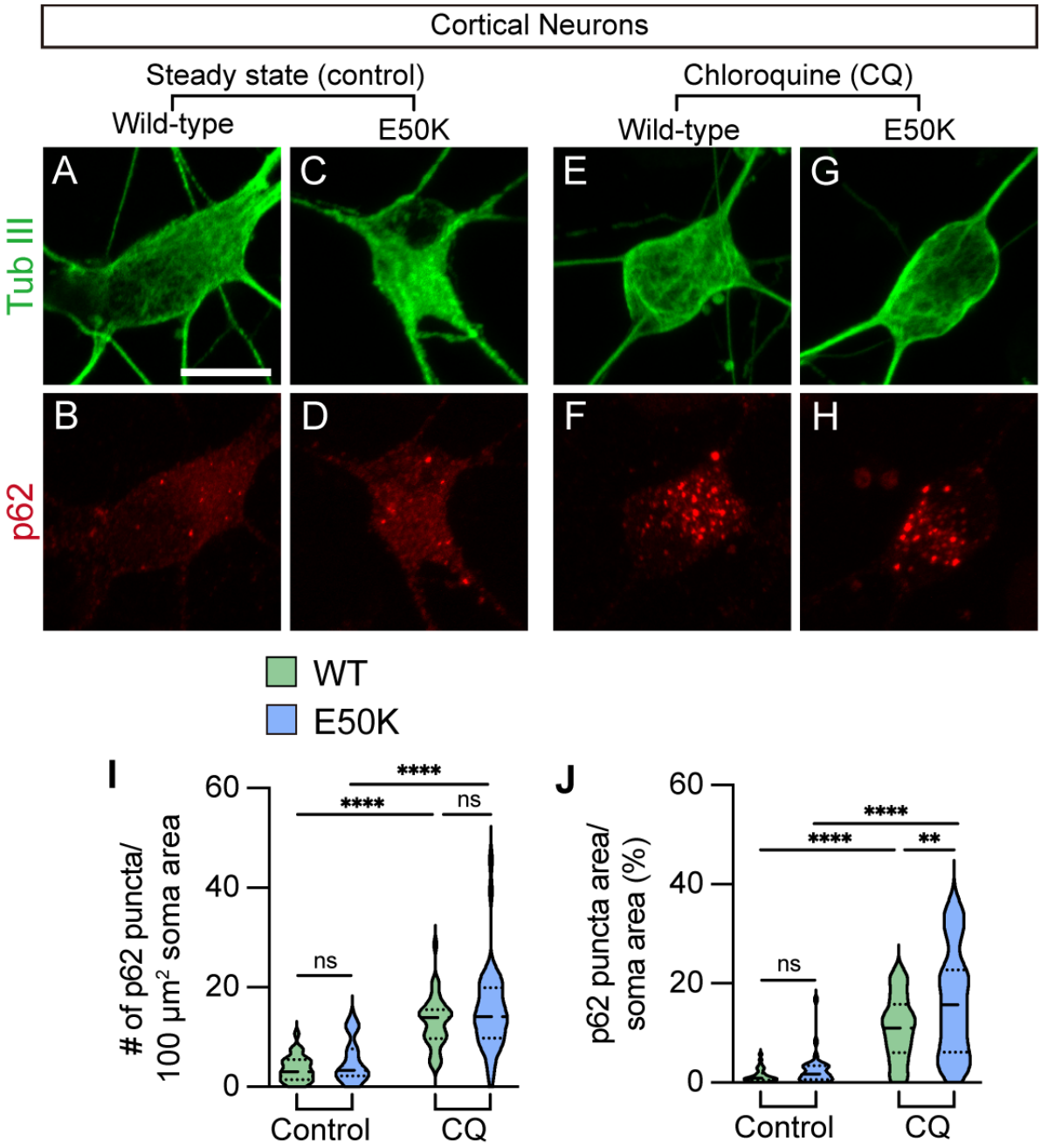

Figure S8. Characterization of p62 expression in hPSC-cortical neurons from wild-type and OPTN(E50K) cell lines.

(**A-H**) Representative images of p62 puncta in iPSC-derived cortical neurons from WT and OPTN(E50K) cell lines under steady state (control) (A-D) and chloroquine (CQ) treatment (E-H). Scale bar: 10 µm. (**I-J**) Quantification of p62 puncta in iPSC-derived cortical neurons (n=3 biological replicates using Ctrl-WT n=30, Ctrl-E50K n=30, CQ-WT n=36 and CQ-E50K n=38 technical replicates; One-way ANOVA, Tukey post hoc test. ****p<0.0001, **p<0.01, ns= not significant, p>0.05). Data are all represented as mean values ± SEM.

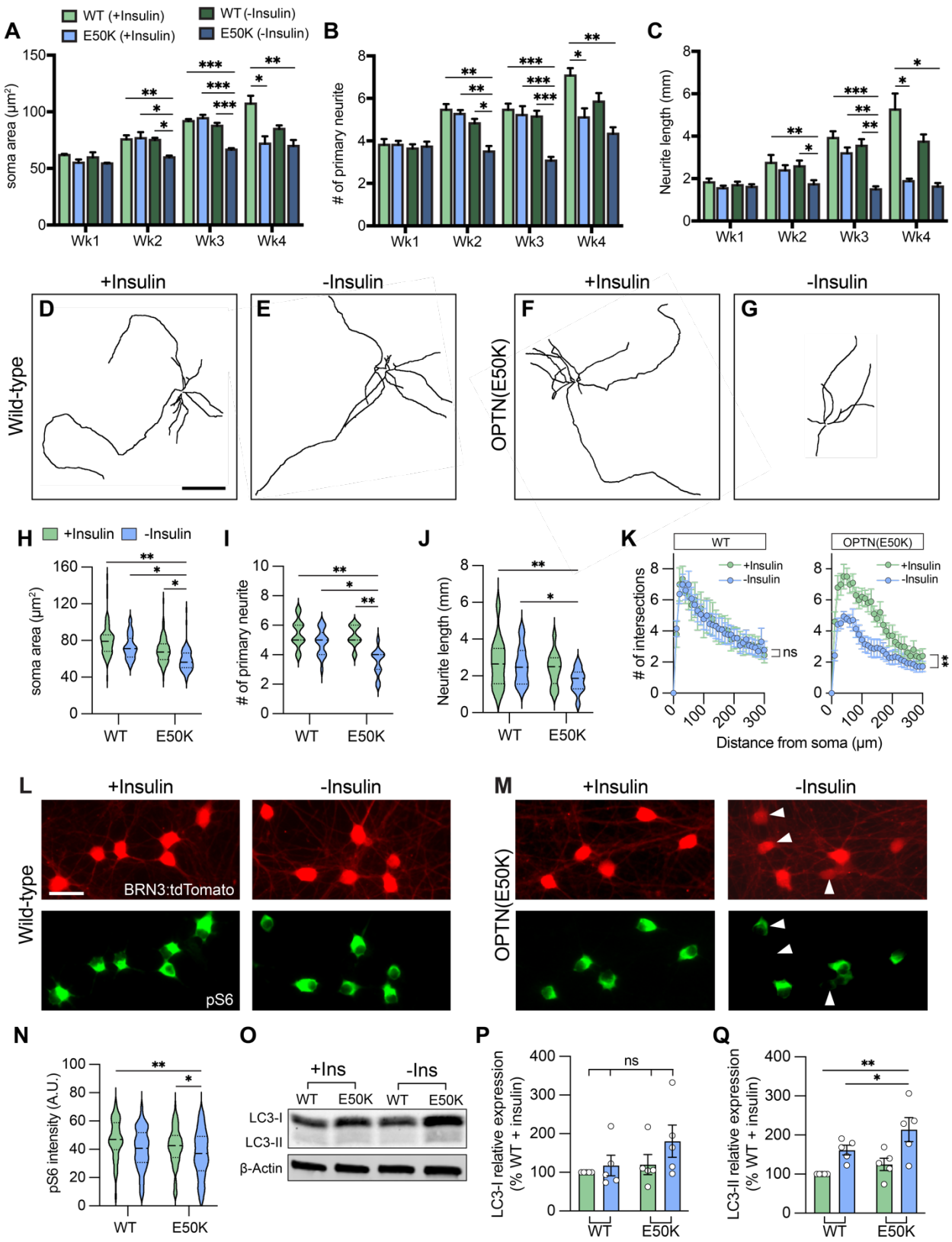

Figure S9. Insulin deprivation accelerated hPSC-RGCs neurite deficits under OPTN(E50K) mutation.

(**A-C**) Quantitative analysis of neurite measurements over the course of 4 weeks of differentiation in wild-type and OPTN(E50K) hPSC-RGCs grown with or without insulin, as measured by soma size (n≥30 each condition with 4 biological replicates; One-way ANOVA, Tukey post hoc test. ***p<0.001, **p<0.01, *p<0.05) (A), number of primary neurites (n≥10 each condition with 4 biological replicates; One-way ANOVA, Tukey post hoc test. ***p<0.001, **p<0.01, *p<0.05) (B), total neurite length (n≥10 each condition with 4 biological replicates; One-way ANOVA, Tukey post hoc test. ***p<0.001, **p<0.01, *p<0.05) (C). (**D-G**) Representative neurite tracings of WT and OPTN(E50K) hPSC-RGCs after 2 weeks of growth either with insulin or without insulin. Scale bar: 200 µm. (**H-K**) Quantitative analysis of neurite parameters identified neurite deficits in OPTN(E50K) hPSC-RGCs after insulin deprivation for 2 weeks, as measured by their soma size (n=4 biological replicates using WT(+Ins) n=103, E50K(+Ins) n=91, WT(-Ins) n=74, and E50K(-Ins) n=80 technical replicates; One-way ANOVA, Tukey post hoc test. **p<0.01, *p<0.05) (H), number of primary neurites (n=4 biological replicates using WT(+Ins) n=13, E50K(+Ins) n=15, WT(-Ins) n=17, and E50K(-Ins) n=12 technical replicates; One-way ANOVA, Tukey post hoc test. **p<0.01, *p<0.05) (I), total neurite length (n=4 biological replicates using WT(+Ins) n=13, E50K(+Ins) n=13, WT(-Ins) n=14, and E50K(-Ins) n=11 technical replicates; One-way ANOVA, Tukey post hoc test. **p<0.01, *p<0.05) (J), and Sholl analysis (n=3 biological replicates using WT(+Ins) n=9, E50K(+Ins) n=10, WT(-Ins) n=13, and E50K(-Ins) n=14 technical replicates; t-test, WT(+Ins) vs WT(-Ins): ns= not significant, p=0.73; E50K(+Ins) vs E50K(-Ins): ***p=0.0004) (K). (**L-M**) Immunostaining revealed that a subset of OPTN(E50K) hPSC-RGCs reduced their expression of $pS6^{Ser240/244}$ when cultured under insulin deprivation, while wild-type RGCs did not change $pS6^{Ser240/244}$ expression under these experimental parameters. Scale bar: 25 µm. (**N**) Quantification of $pS6^{Ser240/244}$ intensity indicated the decrease of mTORC1 levels in OPTN(E50K) hPSC-RGCs after insulin deprivation (n=3 biological replicates using WT(+Ins) n=119, E50K(+Ins) n=117, WT(-Ins) n=118, and E50K(-Ins) n=126 technical replicates; One-way ANOVA, Tukey post hoc test. **p<0.01, *p<0.05). (**O-Q**), Western blot and quantification of the relative protein expression demonstrated the increased expression of LC3-II in OPTN(E50K) hPSC-RGCs following insulin deprivation for only two weeks (n=5 for each group; One-way ANOVA, Tukey post hoc test. **p<0.01, *p<0.05, ns= not significant, p>0.05). Data are all represented as mean values ± SEM.

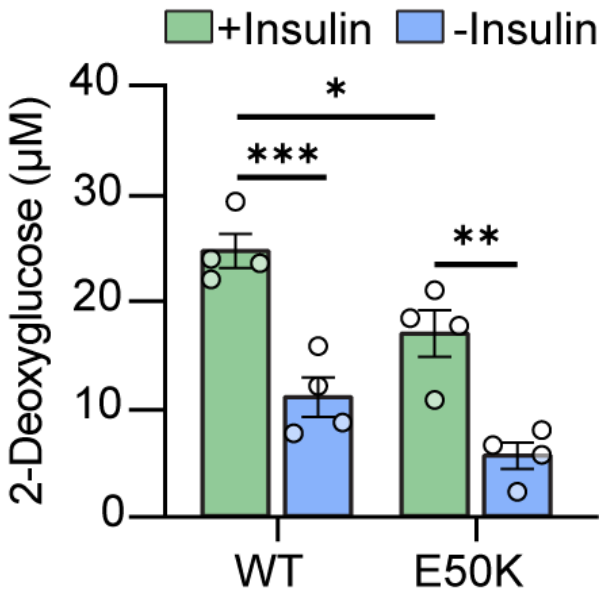

Figure S10. Insulin deprivation induces glucose uptake deficits in both WT and OPTN(E50K) RGCs. Bar graphs represent the concentration of 2-Deoxyglucose (2-DG) uptaken by WT and OPTN(E50K) RGCs grown with or without insulin. Reduced levels of 2-DG uptake were observed in OPTN(E50K) RGCs compared to isogenic control indicating deficits in glucose uptake by glaucoma-associated RGCs. Moreover, reduced levels of uptaken 2-DG were also observed in both WT and OPTN(E50K) grown without insulin compared to the genotype incubated with media containing insulin, suggesting the insulin deprivation induces glucose uptake deficits in RGCs. Data represents mean values ± SEM, from four biological replicates. *p<0.05, **p<0.01 and ***p<0.001, one-way ANOVA followed by Šídák's multiple comparison test with selected pairs.